The International Journal of Advanced Manufacturing Technology
https://doi.org/10.1007/s00170-019-03396-9

ORIGINAL ARTICLE

Evaluation of the impact of scanning strategies on residual stresses in selective laser melting

L. Mugwagwa[1] · D. Dimitrov[1] · S. Matope[1] · I. Yadroitsev[2]

Received: 22 November 2018 / Accepted: 23 January 2019

Abstract

The occurrence of residual stresses in selective laser melting (SLM) presents challenges that limit the capability of the process to manufacture parts at industrial scale. These stresses can have irreversible effects such as warping and cracking of parts during and post manufacturing. One of the most important SLM parameters that should be controlled carefully in order to effectively manage residual stresses is the scanning strategy. This study presents an evaluation of four different scanning strategies, namely the island, successive, successive chessboard and least heat influence (LHI) scanning strategies with respect to their influence on residual stresses and distortions. All the scanning strategies were investigated by melting single tracks on tool steel substrates without powder. Measurement of residual stresses was performed on selected positions on the substrates before and after exposure to the laser beam using the x-ray diffraction technique. The successive chessboard scanning strategy was found to contribute to the least average residual stresses, and lowered residual stress by up to 40% relative to the default island scanning strategy. Further to this, the influence of the successive chessboard and island scanning strategies on distortions was evaluated. Similar to the residual stress findings, the successive chessboard contributed to lower form deviations compared to the island strategy. The scanning strategies were also evaluated based on their impact on total scanning times, with the successive chessboard strategy showing slightly lower scanning time than that for the island and LHI chessboard strategies.

Keywords Selective laser melting · Scanning strategies · Residual stresses · X-ray diffraction

1 Introduction

Selective laser melting (SLM) is a powder bed fusion process which enjoys widespread application in die- and mould-making industry as well as for manufacture of bone implants. Other areas of application include the automotive, aerospace and consumer goods sectors. SLM offers nearly unlimited design freedom and is capable of achieving mechanical/physical properties such as hardness and density that compare well to those obtained from conventional manufacturing processes such as forging. Regardless, limitations such as residual stresses that arise from high thermal gradients and non-uniform heating and cooling still persist. Residual stresses often lead to cracking, delamination, form distortions as well as accelerated in-service fatigue failure. Residual stresses can lead to warping of the part under fabrication, and sometimes even the baseplate. The most severe cases of stress-induced warping necessitate stoppage or abortion of the build. It is, therefore, important to develop mechanisms to reduce residual stresses and their effect, both during and after SLM. Some of the common residual stress management methods include preheating of the baseplate and/or powder bed, rescanning the powder bed, post process heat treatment and scanning strategy improvements.

Preheating the powder bed reduces the temperature difference between the melt pool and surrounding powder, leading to reduction of residual stresses [1]. A study by Ali et al. [2] shows a general decline in residual stresses with increase in powder bed (preheat) temperature for Ti6Al4V. In another study, preheating the powder bed to 150 °C improved the dimensional accuracy of 316L stainless steel tensile test specimens by 10% [3]. Shiomi et al. [4] posted a 40% decrease in

✉ L. Mugwagwa
lameck@sun.ac.za

[1] Stellenbosch Technology Centre – Laboratory for Advanced Manufacturing, Department of Industrial Engineering, Stellenbosch University, Stellenbosch 7602, South Africa

[2] Centre for Rapid Prototyping and Manufacturing, Department of Mechanical and Mechatronic Engineering, Central University of Technology, Bloemfontein 9300, South Africa

Published online: 01 February 2019

residual stresses when the baseplate was preheated to 160 °C. Kempen et al. [5] used preheating temperatures of 90 °C, 150 °C and 200 °C to demonstrate that increasing the preheating temperature of the baseplate progressively reduces stress-related cracking and delamination in SLM of M2 HSS parts. Similarly, Furumoto et al. [6] achieved a residual stress reduction from around 1000 MPa (without baseplate preheating) to 200 MPa (with baseplate preheating). The results presented by Roberts [7] for SLM of Ti6Al4V show that increasing the building chamber preheating temperature from 40 to 300 °C yields about 50% reduction in residual stresses in Ti6Al4V.

Another approach to residual stress management is rescanning whereby the laser beam scans the powder bed "*n*" times (usually twice). Rescanning acts as a form of heat treatment that relieves thermal stresses that could have been set up during the initial pass. This strategy was investigated by Becker and Dimitrov [8] as well as Shiomi et al. [4], with latter reporting up to 55% reduction of residual stresses. Mercelis and Kruth [9] showed that rescanning the 316L stainless steel powder bed at an energy density of 50% of the initial pass results in reduction of residual stresses in the range of 30% compared to when no rescanning is performed. The apparent challenges that come with residual stress management methods such as preheating and rescanning are to do with energy efficiency [10]. Furthermore, rescanning increases the building time (and total manufacturing cost). Heat treatment is also very effective, with up to 70% reduction of residual stresses being reported by Shiomi et al. [4]. Stress-relief annealing is also commonly used to reduce residual stresses in finished parts, and this can be carried out whilst the built parts are still attached to the build platform [11–13]. The limitation of post process heat treatment is its inability to reverse the effects of residual stresses on distortions, delamination and stress-related cracking that occurs during manufacturing.

One of the most attractive in situ residual stress management approaches that can effectively reduce both residual stresses and distortion of final parts is scanning strategy improvement. Scanning strategy refers to the pattern (or path) in which the laser is moved over the powder bed to effect melting. Besides having a direct influence on residual stresses, scanning strategies determine several other outcomes such as tensile properties, achievable density, microstructure and surface finish [14–16]. Several researchers have studied a number of scanning strategies to establish how these strategies influence residual stresses in SLM manufactured parts. Jhabvala et al. [17] used four different scanning strategies to study the effects of these strategies on heating homogeneity. They conclude that the parallel and spiral scanning strategies contribute to large thermal gradients and that subdividing the area to be scanned by adopting the paintbrush or the chessboard scanning strategies result in more homogeneous heating of the powder bed, which reduces thermal stresses. Kruth et al. [18] studied the effect of scan vector length with results showing a decrease of residual stress-related deformations with decrease in the scan vector length. For a vector length of 10 mm, the curl up angle of Ti6Al4V bridges was approximately 12% higher than that for a scan vector of 2.5 mm. Töppel et al. [19] compared the strip scanning strategy to the chessboard strategy and their results show that residual stresses decreased from about 150 MPa when using the strip strategy to about 115 MPa when using the chessboard strategy. Zaeh and Branner [20] investigated the effect of four different scanning strategies on residual stresses. From their findings, it was evident that the island strategy, which consistently employs the shortest scan vectors, by far contributed to the least residual stresses. Wu et al. [21] report decrease of residual stress when the island size (of the island scanning strategy) is reduced from 5 mm × 5 mm to 3 mm × 3 mm. Li et al. [22] presented a comparison of 4 scanning strategies—horizontal sequential, vertical sequential, successive and least heat influence (LHI) strategy. Their conclusion is that the successive and LHI strategies (which make use of shorter vector lengths) show better potential of reducing residual stresses when compared to sequential strategies. In summary, there seems to be a consensus from previous researches that reducing the scan vector length, through sub-division of the region to be scanned, is effective in reducing the magnitude of generated thermal stresses. However, limited research is available on the effect of scanning sequences for the sub-sections on residual stress and associated distortions, as well as on production rates. Thus, this paper presents the development and evaluation of different SLM scanning strategies with respect to residual stresses, distortions and productivity.

2 Methodology

The study method involved developing and selecting scanning sequences for experimental investigation. The experimental investigations focused on the impact of the different scanning sequences on residual stresses, distortions and productivity. A general flow of the investigation approach is illustrated in Fig. 1.

2.1 Scanning strategy selection

Based on the background which clearly demonstrates the superiority of strategies that employ short scan vectors, this study presents scanning pattern variations in which, for every slice, the shape to be scanned is divided into smaller subsectors. For all the scanning strategies under investigation, the scan vectors are rotated by 90° between adjacent subsectors as shown in Fig. 2. Although the scan vector angle is also influential in determining residual stresses emanating from different scanning strategies, this is not investigated in

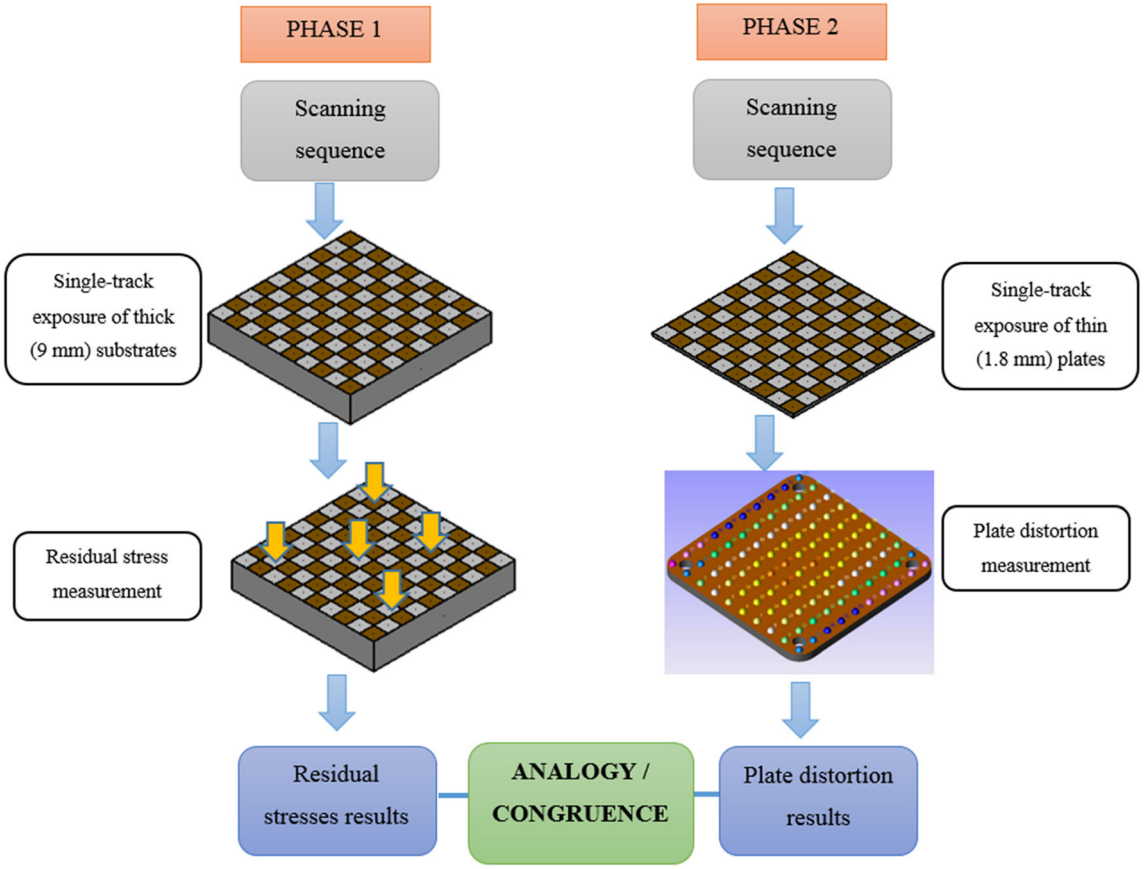

Fig. 1 Study methodology flow diagram

this paper. Therefore, the scan vector angle was maintained at 90° (or 0°) for all the scanning sequences investigated. The difference in the scanning strategies studied lies in the sequence of scanning the sub-sectors. To study the effect of different patterns for scanning the sub-sectors, also called "islands" herein, four scanning strategies were considered. All the islands were maintained at 5 mm × 5 mm for all the strategies investigated.

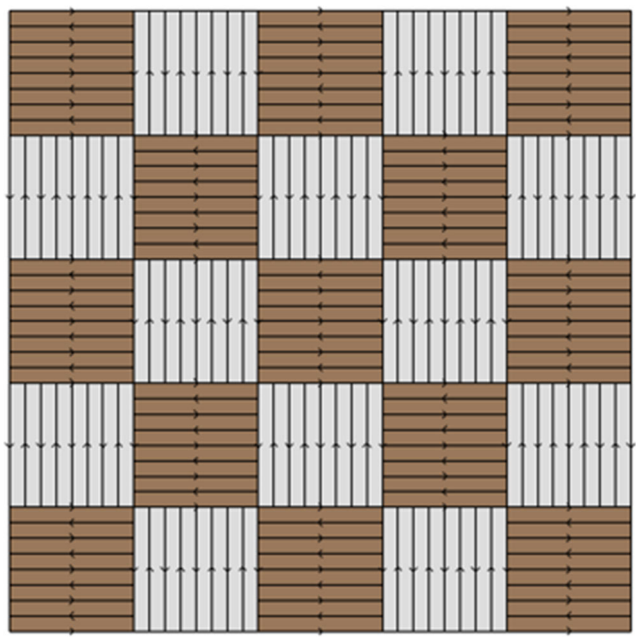

Fig. 2 Scan vector orientation between adjacent islands

The first strategy considered in this paper is Concept Laser's island scanning strategy in which sub-divisions (islands) are scanned in a random manner [23]. The randomness in the exposure of the islands makes this strategy similar to the chessboard described by Jhabvala et al. [17]. The island scanning strategy is the default scanning strategy on the M2 Laser Cusing machine utilised for this study. The second strategy, named "*successive* scanning strategy" involves scanning of the sub-sectors directly one after the other as shown in Fig. 3b. The difference in the colour of the sub-divisions (light and dark) represents the 90° rotation of scan vector directions between neighbouring sub-sectors as explained earlier in Fig. 2. This strategy was previously studied by Li et al. [22] and Kruth et al. [24].

For the third scanning strategy, an approach in which the sub-sectors are scanned in a chessboard fashion is proposed. The sub-sectors with horizontal scan vectors are successively scanned first before the vertical vector sectors can be scanned, or vice versa. This strategy will be referred to as the "*successive chessboard* scanning strategy" and is shown in Fig. 3c. A similar strategy was investigated by Ali et al. [25]. Lastly, a

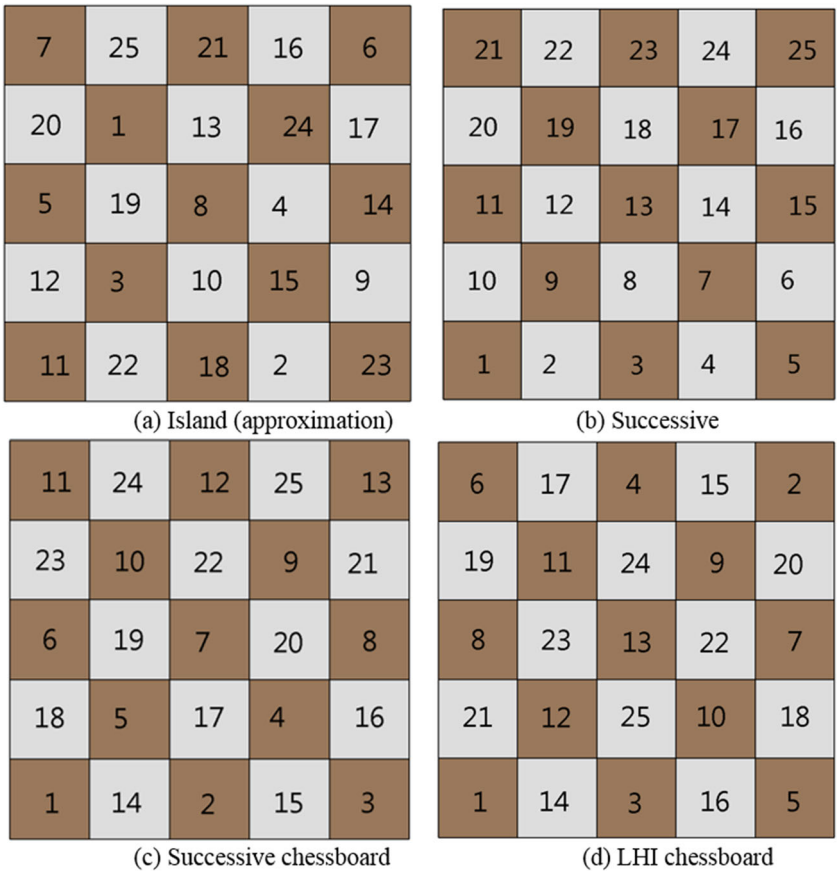

Fig. 3 Illustration of typical scanning sequences for the different scanning strategies investigated. **a** Island (approximation). **b** Successive. **c** Successive chessboard. **d** LHI chessboard

variation of the successive chessboard strategy is considered in which the next sector to be scanned lies as far as possible from the current sub-sector. This strategy will be identified as the "*Least Heat Influence (LHI)* chessboard scanning strategy" and is illustrated in Fig. 3d. For this scanning strategy, a literal chessboard style is followed, thereby distinguishing it from LHI strategies discussed by Li et al. [22] and Kruth et al. [24]. Furthermore, the scan vectors were not necessarily rotated between adjacent islands in the implementation of the LHI by Li et al. [22]. Although the random nature of the island strategy is somewhat similar to the LHI pattern, a major standout difference is in that the island strategy does not utilise the chessboard approach of scanning the light islands first before the dark islands or vice versa. Figure 3 shows all the four scanning strategies that were compared.

2.2 Influence of scanning sequence on residual stresses and distortions

The influence of scanning strategies on residual stresses was investigated by exposing AISI H13 hot work tool steel substrates to a 180 W laser without metal powder, at a scanning speed of 600 mm/s. At 9 mm thick, the substrates were considered stiff enough to resist any stress-related warping after interaction with the laser beam. Use of thinner plates would have resulted in warping and potentially distort the interpretation of residual stress results since warping leads to stress relief and/or redistribution. Before exposure to the laser beam, a section of the tool steel substrate was evaluated for surface residual stresses at three randomly chosen points. This initial stress state was taken into account for calculating the actual residual stress magnitude associated with the laser melting for the different scanning strategies. Previous studies on residual stresses in SLM [26] show that different positions at the same measurement depth can have different residual stress magnitudes. Thus, it is essential to measure on more than one point on the surface in order to draw accurate conclusions. After laser beam exposure, five measurement positions on the melted surface were selected for residual stress evaluation as shown in Fig. 4a. These points were carefully selected to ensure the entire baseplate area is adequately represented. For each of the five points on the baseplate after exposure, measurements were done at the centre of each "island" along (longitudinal) and perpendicular (transverse) to the scanning direction. Figure 4b is an image of the actual melted area on the baseplate. Here, the chessboard style is clearly depicted.

Residual stresses were evaluated using the x-ray diffraction (XRD) technique. A Proto XRD machine was utilised for this purpose. The principle of the XRD method is that when irradiated x-rays penetrate a material, the crystal planes of the

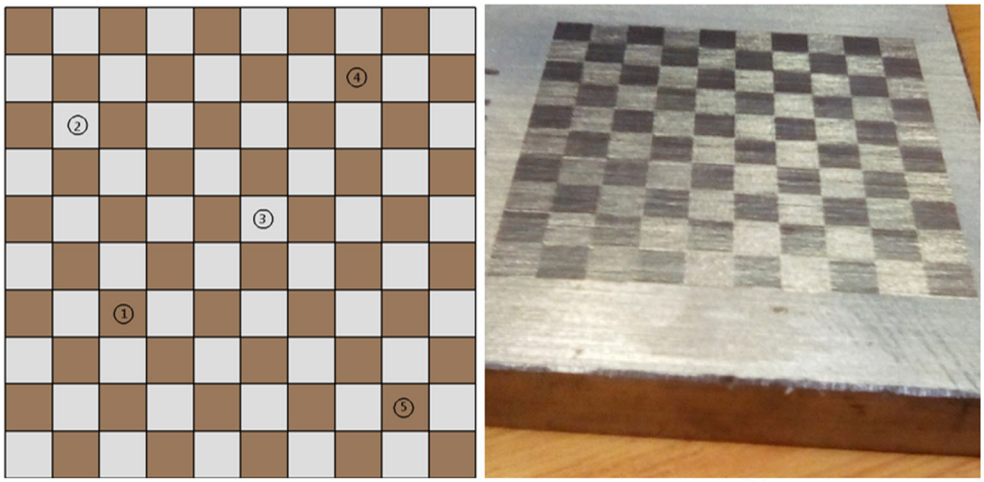

Fig. 4 **a** XRD measurement points and **b** image of the laser melted region on the substrate

material will diffract some of these rays. Using a detector, the angular positions of these diffracted rays are detected and their intensity at these positions is recorded. These positions are compared to the original or stress-free positions and, using Bragg's law, the new lattice spacing (d-spacing) is calculated, and the strains that resulted from the deformations are also evaluated [27]. For this work, a Proto XRD x-ray diffractometer equipped with two detectors was utilised to determine the Fe-α {211} lattice deformations at 25 kV and 4 mA. The source of x-rays was a Cr K-α x-ray anode tube, at a wavelength of 2.291 Å as recommended in Fitzpatrick et al. [28]. The $\sin^2\psi$ method [28, 29] was used to calculate the stress. This method, involves plotting a graph of d-spacing, d, against $sin^2\psi$ and using the gradient of this plot in calculating the residual stress, σ, as given in Eq. 1 [28]. It is essential to ensure that specimen surfaces are clean since contaminants can easily lead to measurement errors. Thus, the substrates were stored in sealed containers immediately after laser melting in order to minimise oxidation of surfaces.

$$\sigma = \left(\frac{E}{1+v}\right)m \tag{1}$$

where E is the material's modulus of elasticity, v is the Poisson's ratio and m is the gradient of the plot. Details of the derivation of the $\sin^2\psi$ method can be found in Fitzpatrick et al. [28].

The effect of scanning strategies on residual stresses was verified by extending the study to investigate how these scanning strategies influence residual stress-induced distortions. This was achieved by investigating the deformation that 1.8-mm-thick plates of grade 5 titanium alloy would experience upon exposure to the laser beam. Single track experiments were conducted by exposing the thin metal plate, acting as the baseplate, to the laser beam without application of metal powder. Thin plates are easily susceptible to warping under thermal stress, making it possible to measure the warping deviation and correlating the same to the previously measured residual stresses as seen from a similar study by Li et al. [22]. This is an indirect but effective method of evaluating or modelling the effect of residual stresses on distortions. The distortions in this study were measured using a coordinate measurement machine.

3 Results and discussion

3.1 Effect of scanning strategies on residual stresses

The surfaces of the 9-mm-thick tool steel baseplates were observed to be under a mean compressive residual stress of 450 ± 11 MPa prior to exposure to laser beam. The compressive stress is a direct result of the previous manufacturing processes such as rolling and sandblasting which the baseplates were subjected to. After exposure of the baseplates to the laser beam, the measured residual stress magnitudes (for all cases) were much lower than initial stress state, ranging between − 42 and − 299 MPa. This reduction in the compressive stress magnitude is an indication that exposure of the baseplates to the laser beam induced tensile residual stresses. The difference in the stress states before and after exposure was interpreted as the residual stress associated with each specific scanning strategy.

The measured residual stress magnitudes were higher along the longitudinal direction than the transverse. These findings are consistent with previous findings on related research [1, 30, 31]. The successive strategy resulted in the highest mean residual stresses of 348 MPa, measured in the longitudinal direction. It is evident from the results that scanning the subdivisions in direct succession results in non-uniform heat distribution, and possibly leads to overheating. In comparison,

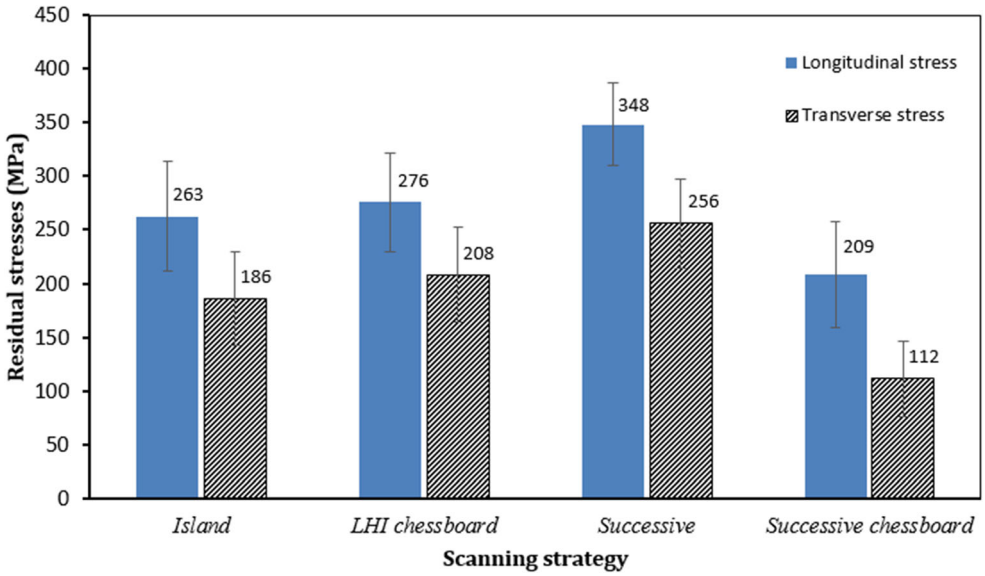

Fig. 5 Residual stress results for the different scanning strategies

the island and the LHI chessboard strategies contributed to lower mean stress magnitudes of 263 MPa and 276 MPa respectively. More uniform heating and solidification is achieved when these strategies are implemented, as opposed to the successive scanning strategy. Although the island and LHI scanning strategies are different in principle, observation during the actual scanning showed that the randomness of the island strategy in selecting the next island to scan is actually very much similar to that of the LHI chessboard. This explains the similarities in the measured residual stress values for the two scanning strategies. Of interest is the successive chessboard strategy, which contributes to the least average stress of 209 MPa as shown in Fig. 5. The amassing of heat described in Li et al. [22] and Kruth et al. [24] appears to play a role. Heat amassing, which is higher for the successive chessboard strategy compared to the LHI and the island strategies, helps reduce the temperature differences between adjacent sub-sectors, leading to the observed reduction of the resulting stresses.

3.2 Effect of scanning strategies on distortions

After the evaluation of residual stresses for the different scanning strategies investigated, the island and the successive chessboard scanning strategies were further evaluated to establish their effect on distortions. Prior to laser beam exposure, the titanium plates were checked for flatness in order to ensure that any warping distortion observed after melting can be solely attributed to residual stress-induced deformation. The plates were satisfactorily flat, showing no sign of warping or waviness of the surface, with an average deviation of 0.004 mm. Thereafter, an EOSINT M280 machine was utilised to melt the surfaces of 1.8-mm grade 5 titanium plates without any deposition of powder. As a control, the default scanning strategy on the EOSINT M280 machine, the stripe hatch, was also evaluated, although this strategy had not initially been evaluated for residual stresses. The stripe hatch strategy, referred to as the paintbrush strategy by Jhabvala et al. [17], is illustrated in Fig. 6. Laser power, scanning speed and hatch spacing were set to 170 W, 1200 mm/s and 100 μm respectively.

The maximum deviation measured for the successive chessboard strategy was 0.18 mm whilst a maximum of 0.21 mm was found when the "islands" were scanned randomly. These results are consistent with the residual stress findings discussed earlier for these two strategies. On the other hand, the stripe hatch had the largest deviation, reaching a top value of 0.34 mm near the plate edges parallel to the scanning direction. This confirms that reducing short scan vectors indeed improves thermal homogeneity thereby reducing the resulting stresses. On the contrary, stripe hatching tends to concentrate heat on the current strip being melted, resulting in less uniform

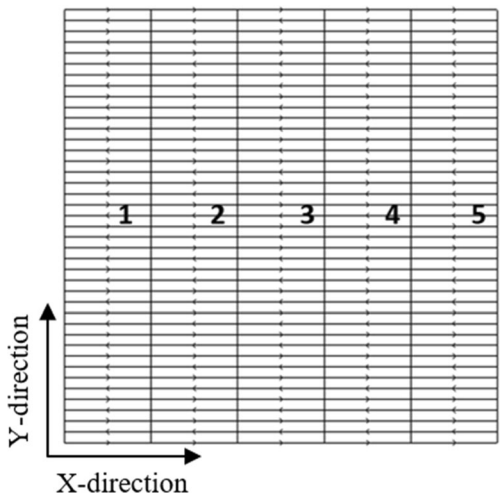

Fig. 6 Stripe hatch strategy

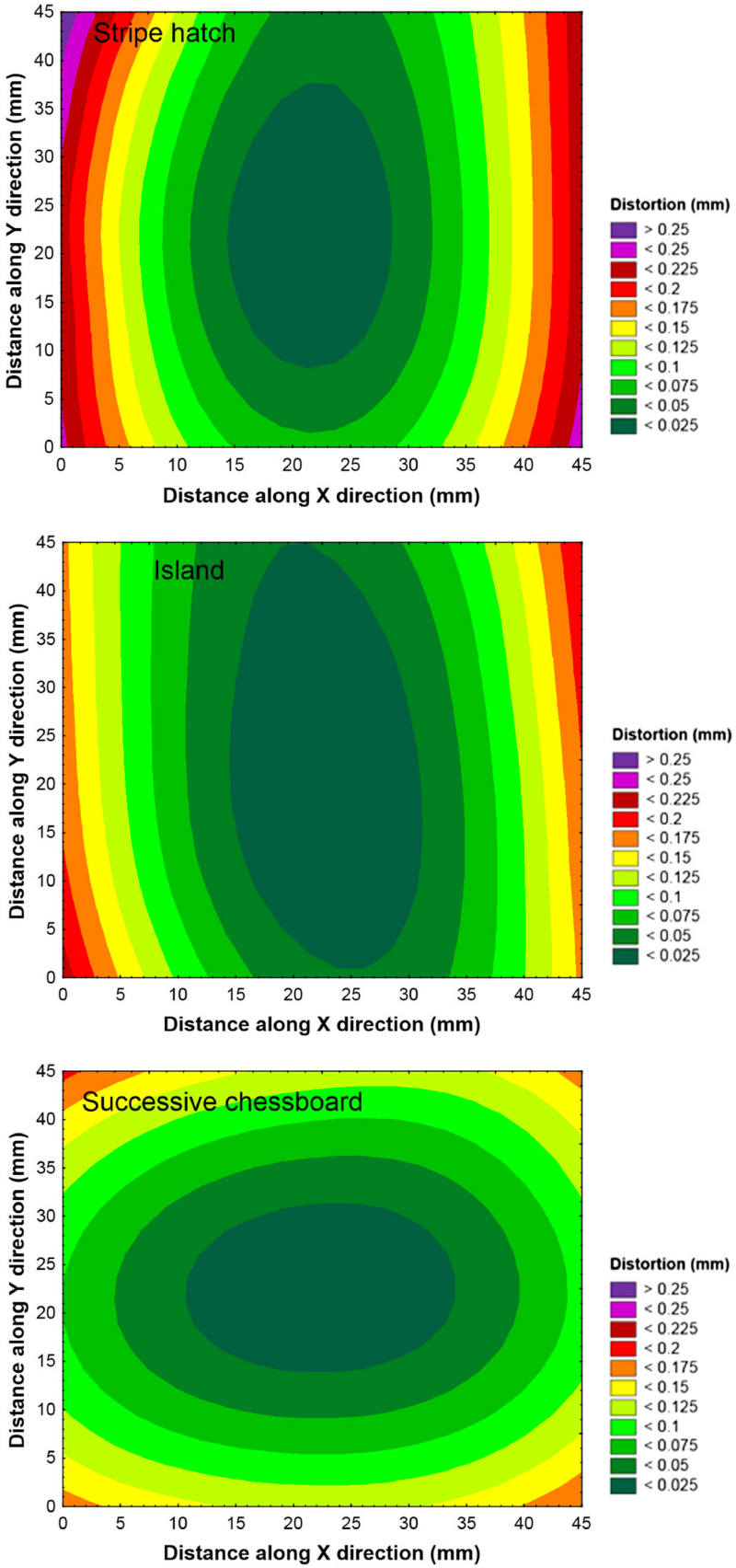

Fig. 7 Distortion of the titanium plates for different strategies investigated

heat distribution across the scanned region's surface area. The differences in the distortion of the plates are illustrated in Fig. 7. On average, the maximum deviations for the successive chessboard, random (island) and stripe hatch strategies were 0.17 mm, 0.20 mm and 0.28 mm respectively. In summary, it has been shown that a structured sequence of exposing the islands results in less residual stresses and associated distortions compared to randomly scanning the sub-divisions. Furthermore, the results are in agreement with other published findings that short scan vectors reduce residual stresses and the associated distortions better than long vectors.

From the residual stress results presented in Fig. 5, and from previous research [30, 32, 33], the residual stress distribution in SLM is highly anisotropic; therefore, rotating of scan vectors between adjacent sub-divisions is also important in minimising this anisotropy. However, such rotation would lead to increase in the scan vector lengths for the stripe hatch strategy. One option to reduce this increase in scan vector length due to rotation would be to use scan vector angles of 45°.

3.3 Effect of scanning strategies on scanning time

The effect of the different strategies on scanning time was evaluated for the island, successive, successive chessboard and LHI chessboard strategies. The lowest scanning time of 40.04 s was recorded for the successive scanning strategy. This can be explained by the elimination of the laser beam "jump" time from sub-sector to sub-sector that is characteristic of all the other 3 strategies. However, the successive scanning strategy yields the highest residual stresses as discussed earlier. On the other hand, the successive chessboard strategy still is superior to the island and LHI chessboard strategies with respect to both residual stresses and scanning time. There is not much difference between the island and the chessboard strategy for both residual stresses and scanning time since they, in practice, follow a very similar exposure sequence. The scanning times for the different scanning strategies are summarised in Table 1 for the 50 mm × 50 mm scanning area.

Although the differences in the scanning times for the different strategies are only fractions of a second, they still impact on total building time especially with increase in consolidation height and for parts that cover a substantial area on the baseplate. For example, a building height of 45 mm translates to 1500 layers for a layer thickness on 30 μm. For the process settings used in this paper, the corresponding scanning times for the different scanning strategies would be as given in Table 2. The time savings become apparent as the number or volume of parts consolidated increases. According to a study by Rickenbacher et al. [34], the scanning time contributes about 77% of the total time to build up parts. Furthermore, the cost of building is directly proportional to the building time as modelled in Eq. 2 [34]. Cutting on building time reduces the operational costs related to inert gas, energy and labour. In turn, this would result in reduction of the total manufacturing cost.

Table 1 Scanning times associated with the different scanning strategies

Scanning strategy	Scanning time (s)
Island	40.54
Successive	40.04
Successive chessboard	40.16
LHI chessboard	40.68

Table 2 Estimated scanning times for 50 mm × 50 mm × 45 mm parts and time savings against the island strategy

Scanning strategy	Scanning time per part (s)	Time savings per part (s)
Island	60,810	–
Successive	60,060	+ 750
Successive chessboard	60,240	+ 570
LHI chessboard	61,020	− 210

$$C_{\mathrm{Bld}}(P_i) = T_{\mathrm{Bld}}(P_i)*\left(C_{\mathrm{Mchn}} + C_{\mathrm{gas}}\right) + V(P_i)*C_{\mathrm{Mat}} \qquad (2)$$

where C_{Bld} is the cost of building the part; P_i is part with ith geometry; T_{Bld} is the building time (hours); $V(P_i)$ is the volume of the part (mm^3); and C_{Mchn}, C_{gas} and C_{Mat} represent the machine cost (per hour), cost of inert gas consumption (per hour) and material cost (per kg) respectively [34].

4 Conclusion and outlook

In this paper, an overview of residual stress management strategies was discussed, leading to comparison of different scanning patterns with respect to residual stresses and productivity. The following conclusions can be drawn:

- Of the scanning strategies presented in this paper, the successive chessboard strategy is the most attractive since it results in the least residual stresses. On the other hand, scanning sub-sectors directly one after the other contribute to the highest residual stresses due to non-uniform heating and cooling across the powder bed. The effect of the strategies on distortions shows that the successive chessboard is superior to the island strategy, in agreement with the residual stress results. At the same time, the stripe hatch leads to significant warping along the scanning direction.

- The implementation of the island and LHI chessboard strategies is quite similar. Hence, their effect on heat distribution across the powder bed, and consequently on residual stresses, is somewhat comparable.
- The different scanning strategies show slight differences in the scanning times, with the successive strategy having the lowest scanning time per layer. However, these differences in scanning time can have a major impact on the build time for wider and thicker parts, and when building several parts on one platform as shown in this paper.
- The findings in this paper can be extended to modelling and experimental validation of the implication of scanning strategies on total manufacturing cost.

Acknowledgements The authors are grateful to the National Research Foundation of South Africa for supporting this research. Many thanks to the staff at Nelson Mandela University for their assistance with XRD measurement of residual stresses.

Funding information The Department of Science and Technology of South Africa is acknowledged for the funding under the Collaborative Programme on Additive Manufacturing.

References

1. Gusarov AV, Pavlov M, Smurov I (2011) Residual stresses at laser surface remelting and additive manufacturing. Phys Procedia 12: 248–254. https://doi.org/10.1016/j.phpro.2011.03.032.
2. Ali H, Ma L, Ghadbeigi H, Mumtaz K (2017) In-situ residual stress reduction, martensitic decomposition and mechanical properties enhancement through high temperature powder bed pre-heating of selective laser melted Ti6Al4V. Mater Sci Eng A 695:211–220. https://doi.org/10.1016/j.msea.2017.04.033
3. Zhang B, Dembinski L, Coddet C (2013) The study of the laser parameters and environment variables effect on mechanical properties of high compact parts elaborated by selective laser melting 316L powder. Mater Sci Eng A 584:21–31. https://doi.org/10.1016/j.msea.2013.06.055
4. Shiomi M, Osakada K, Nakamura K, Yamashita T, Abe F (2004) Residual stress within metallic model made by selective laser melting process. CIRP Ann 53:195–198. https://doi.org/10.1016/S0007-8506(07)60677-5
5. Kempen K, Thijs L, Vrancken B, Buls S, Van Humbeek J, Kruth J-P (2013) Lowering thermal gradients in selective laser melting by pre-heating the baseplate. In: Solid Freeform Fabrication Symposium, Austin, pp 131–139. https://core.ac.uk/download/pdf/34572651.pdf
6. Furumoto T, Ueda T, Abdul Aziz M, Hosokawa A, Tanaka R (2010) Study on reduction of residual stress induced during rapid tooling process: influence of heating conditions on residual stress. Key Eng Mater 447–448:785–789. https://doi.org/10.4028/www.scientific.net/KEM.447-448.785
7. Roberts IA (2012) Investigation of residual stresses in the laser melting of metal powders in additive layer manufacturing, PhD Thesis, University of Wolverhampton
8. Becker T, Dimitrov D (2016) The achievable mechanical properties of SLM produced Maraging Steel 300 components. Rapid Prototyp J 22:487–494. https://doi.org/10.1108/RPJ-08-2014-0096
9. Mercelis P, Kruth J (2006) Residual stresses in selective laser sintering and selective laser melting. Rapid Prototyp J 12:254–265. https://doi.org/10.1108/13552540610707013
10. Papadakis L, Chantzis D, Salonitis K (2018) On the energy efficiency of pre-heating methods in SLM/SLS processes. Int J Adv Manuf Technol 95:1325–1338. https://doi.org/10.1007/s00170-017-1287-9
11. Pupo Y, Delgado J, Serenó L, Ciurana J (2013) Scanning space analysis in selective laser melting for CoCrMo powder. Procedia Engineering 63:370–378. https://doi.org/10.1016/j.proeng.2013.08.228
12. Manfredi D, Calignano F, Krishnan M, Canali R, Ambrosio E, Atzeni E (2013) From powders to dense metal parts: characterization of a commercial AlSiMg alloy processed through direct metal laser sintering. Materials 6:856–869. https://doi.org/10.3390/ma6030856
13. Sames WJ, List FA, Pannala S, Dehoff RR, Babu SS (2016) The metallurgy and processing science of metal additive manufacturing. Int Mater Rev 61:1–46. https://doi.org/10.1080/09506608.2015.1116649.
14. Bo Q, Yu-sheng S, Qing-song W, Hai-bo W (2012) The helix scan strategy applied to the selective laser melting. Int J Adv Manuf Technol 63:631–640. https://doi.org/10.1007/s00170-012-3922-9
15. King WE, Anderson AT, Ferencz RM, Hodge NE, Kamath C, Khairalla SA, Rubenchik AM (2015) Laser powder bed fusion additive manufacturing of metals; physics, computational, and materials challenges. Appl Phys Rev 2:041304. https://doi.org/10.1063/1.4937809
16. Thijs L, Verhaeghe F, Craeghs T, Van Humbeeck J, Kruth JP (2010) A study of the microstructural evolution during selective laser melting of Ti-6Al-4V. Acta Mater 58:3303–3312. https://doi.org/10.1016/j.actamat.2010.02.004
17. Jhabvala J, Boillat E, Antignac T, Glardon R (2010) On the effect of scanning strategies in the selective laser melting process. Virtual Phys Prototyp 5:99–109. https://doi.org/10.1080/17452751003688368
18. Kruth J-P, Deckers J, Yasa E, Wauthle R (2012) Assessing and comparing influencing factors of residual stresses in selective laser melting using a novel analysis method. Proc Inst Mech Eng B J Eng Manuf 226:980–991. https://doi.org/10.1177/0954405412437085
19. Töppel T, Müller B, Hoeren KPJ, Witt G (2016) Eigenspannungen und verzug bei der additiven fertigung durch laserstrahlschmelzen. Schweissen Und Schneiden 68:176–186
20. Zaeh MF, Branner G (2010) Investigations on residual stresses and deformations in selective laser melting. Prod Eng 4:35–45. https://doi.org/10.1007/s11740-009-0192-y
21. Wu AS, Brown DW, Kumar M, Gallegos GF, King WE (2014) An experimental investigation into additive manufacturing-induced residual stresses in 316L stainless steel. Metall Mater Trans A Phys Metall Mater Sci 45:6260–6270. https://doi.org/10.1007/s11661-014-2549-x
22. Li C, Fu CH, Guo YB, Fang FZ (2016) A multiscale modeling approach for fast prediction of part distortion in selective laser melting. J Mater Process Technol 229:703–712. https://doi.org/10.1016/j.jmatprotec.2015.10.022.
23. Carter LN, Martin C, Withers PJ, Attallah MM (2014) The influence of the laser scan strategy on grain structure and cracking behaviour in SLM powder-bed fabricated nickel superalloy. J Alloys Compd 615:338–347. https://doi.org/10.1016/j.jallcom.2014.06.172
24. Kruth JP, Froyen L, Van Vaerenbergh J, Mercelis P, Rombouts M, Lauwers B (2004) Selective laser melting of iron-based powder. J

Mater Process Technol 149:616–622. https://doi.org/10.1016/j.jmatprotec.2003.11.051

25. Ali H, Ghadbeigi H, Mumtaz K (2018) Effect of scanning strategies on residual stress and mechanical properties of Selective Laser Melted Ti6Al4V. Mater Sci Eng A 712:175–187. https://doi.org/10.1016/j.msea.2017.11.103
26. Mugwagwa L, Dimitrov D, Matope S, Becker T (2016) A methodology to evaluate the influence of part geometry on residual stresses in selective laser melting. In: International Conference on Competitive Manufacturing, Stellenbosch, pp 133–139. Available at http://scholar.sun.ac.za/handle/10019.1/99209
27. Kandil FA, Lord JD, Fry AT, Grant PV (2001) A review of residual stress measurement methods - a guide to technical selection. NPL Report MATC (A) 4. http://www.npl.co.uk/publications/a-review-of-residual-stress-measurement-methods-aguide-to-technique-selection
28. Fitzpatrick ME, Fry AT, Holdway P, Kandil FA, Shackleton J, Suominen L (2005) Determination of residual stresses by X-ray diffraction. Meas Good Pract Guid 52:1–68
29. Belassel M, Pineault J, Brauss ME (2006) Comparison and evaluation of residual stress measurement techniques, a technical and economical study. In: SEM Annual Conference and Exposition on Experimental and Applied Mechanics, Saint Louis, pp 756–762. http://semimac.org/wp-content/uploads/2015/11/sem.org-2006-SEM-Ann-Confs29p02-Comparison-Evaluation-Residual-Stress-Measurement-Techniques-A.pdf
30. Parry L, Ashcroft IA, Wildman RD (2016) Understanding the effect of laser scan strategy on residual stress in selective laser melting through thermo-mechanical simulation. Addit Manuf 12:1–15. https://doi.org/10.1016/j.addma.2016.05.014.
31. Yadroitsev I, Yadroitsava I (2015) Evaluation of residual stress in stainless steel 316L and Ti6Al4V samples produced by selective laser melting. Virtual Phys Prototyp 10:67–76. https://doi.org/10.1080/17452759.2015.1026045
32. Vrancken B, Cain V, Knutsen R, Van Humbeeck J (2014) Residual stress via the contour method in compact tension specimens produced via selective laser melting. Scr Mater 87:29–32. https://doi.org/10.1016/j.scriptamat.2014.05.016
33. Vrancken B, Wauthle R, Kruth J, Van Humbeeck J (2013) Study of the influence of material properties on residual stress in selective laser melting. In: Solid Freeform Fabrication Symposium, Austin, pp 393–407. http://sffsymposium.engr.utexas.edu/Manuscripts/2013/2013-31-Vrancken.pdf
34. Rickenbacher L, Spierings A, Wegener K (2013) An integrated cost-model for selective laser melting (SLM). Rapid Prototyp J 19:208–214. https://doi.org/10.1108/13552541311312201